ENERGY SEPARATION AND DEMODULATION OF CPM SIGNALS

Balu Santhanam and Malay Gupta

Dept. of E.E.C.E., University of New Mexico
Albuquerque, NM: 87131-1356
Email: bsanthan@eece.unm.edu

ABSTRACT

The Teager-Kaiser energy operator and the related demodulation algorithms are popular schemes for the demodulation of signals that follow the AM–FM model. Traditional applications for these methods include, AM–FM speech analysis/synthesis, image texture analysis or cochannel FM–voice separation. Many of the existing digital modulation schemes such as CPM, CPFSK, FSK, MSK, GMSK and other forms of digital phase modulation that are both bandwidth/power efficient methods for communications can also be formulated in the same AM-FM framework as the energy operator methods. In this paper, we study the application of these energy operator related demodulation techniques to the digital communications problem of demodulating CPM signals and demonstrate their efficacy using 1-REC-CPM and binary modulation.

1. INTRODUCTION

Continuous phase modulation (CPM) and related forms of digital phase modulation such as CPFSK, MSK, GMSK are nonlinear modulation schemes, efficient from both bandwidth and power perspectives. They find widespread use in the wireless/mobile communications infrastructure due to their simple modulator/demodulator structures [1, 2]. While their *instantaneous frequency* (IF) is discrete, their continuous phase produces smaller spectral sidelobes and better spectral efficiency[1]. The optimal detector for CPM demodulation, maximum likelihood detection, however, has significant complexity. Suboptimal alternatives combining polynomial phase modeling and MMSE detection have recently been investigated for CPM demodulation [4].

The Teager-Kaiser energy operator and the related *energy separation algorithm* (ESA) are useful tools for monocomponent AM-FM signal demodulation. The ESA and its discrete-time counterpart (DESA) [6] have been applied to problems of AM-FM speech analysis and synthesis, multidimensional AM–FM analysis, and analog FM-voice separation and demodulation applications [8]. Higher-order versions of the energy operator have been formulated and successfully applied to the problem of multicomponent AM-FM signal separation and demodulation [7, 5].

[1]FSK modulation employs phase discontinuous carrier switching, thereby requiring a larger bandwidth.

CPM and other forms of digital phase modulation, albeit digital modulation, can be reformulated as digital FM modulation and can be cast into the AM-FM signal framework of the energy operator related methods. Recently polynomial phase modeling of the phase of the CPM signal using product higher-order ambiguity functions has been used for CPM demodulation [4]. In this paper, we apply the energy operator related signal processing techniques to the problem of signal separation and demodulation of CPM signals and other related digital phase modulation schemes to provide a suboptimal, yet, computationally simpler alternative to maximum likelihood detection.

2. CPM SIGNAL MODEL

For the purposes of this paper, we will adopt a rectangular pulse-shaping function $p(t)$ with a duration of L symbol periods (L-REC) and binary PAM symbols $a[k] \in \{-1, 1\}$. If $p(t)$ is a raised cosine pulse then this form of CPM is referred to as (L-RAC) CPM. The IF signal in either form of CPM takes the form:

$$\omega_i(t) = \omega_c + 2\pi h \sum_{k=-\infty}^{\infty} a[k]p(t - kT_b),$$

where ω_c is the carrier frequency, h is the FM modulation index and T_b is the bit duration. The phase deviation from the carrier phase is given by:

$$\phi_{\text{dev}}(t; \mathbf{a}) = 2\pi h \sum_{k=-\infty}^{\infty} a[k]q(t - kT_b),$$

where $q(t) = \int_0^t p(\tau)d\tau$ corresponds to the phase pulse shaping function. The CPM signal is then obtained via frequency modulation:

$$r(t) = A\cos\left(\int_{-\infty}^{t} \omega_i(\tau)d\tau + \theta_o\right).$$

Using a pulse shaping function of duration larger than a symbol period will introduce memory into the modulation scheme (LREC-CPM). In this paper, we will focus our attention on the memoryless case with $L = 1$, i.e., (1REC-CPM). Specifically CPM with a rectangular pulse of one symbol duration (1-REC-CPM) is equivalent to continuous phase *frequency shift keying* (CPFSK). Another form of digital modulation, *minimum shift keying* (MSK), is equivalent to 1-REC-CPM with a modulation index of $h = 0.5$, while

0-7803-8116-5/02/$17.00 ©2002 IEEE.

GMSK can also be put into the CPM framework with a Gaussian pulse shaping function [3]. In this paper we will focus our attention on the CPFSK model, i.e., 1-REC-CPM

3. ENERGY DEMODULATION PRIMER

The Teager–Kaiser energy operator is a nonlinear, differential operator that computes the energy of a signal $x(t)$ via:

$$\Psi_c(x) = [\dot{x(t)}]^2 - x(t)\ddot{x(t)},$$

where the dot denotes the time derivative. The discrete–time energy operator applied to the signal $x[n]$ is defined via:

$$\Psi_d(x) = x^2[n] - x[n+1]x[n-1].$$

The *energy separation algorithm* (ESA) developed in [6] uses this operator to separate amplitude modulations from frequency modulations to accomplish monocomponent AM–FM signal demodulation [6]:

$$|a(t)| \approx \frac{\Psi(x)}{\sqrt{\Psi(\dot{x})}}, \quad \omega_i(t) \approx \sqrt{\frac{\Psi(\dot{x})}{\Psi(x)}}.$$

Discrete versions of the ESA (DESA's) [6], the multiband version of the ESA [9] and applications of the ESA to the problems of AM–FM speech analysis–synthesis, AM–FM vocoding, speech formant frequency and formant bandwidth tracking have also been recently investigated [8].

Higher order generalizations of the energy operator, i.e., *higher-order energy operators* (HOEO) for the continuous–time and the discrete–time case are defined via [7, 5]:

$$\begin{aligned} \Upsilon_k(x) &= \dot{x}(t)x^{(k-1)}(t) - x(t)x^{(k)}(t) \\ \Upsilon_k(x) &= x[n]x[n+k-2] - x[n-1]x[n+k-1]. \end{aligned}$$

These operators for sinusoidal input signals measure the higher-order energies of a classical harmonic oscillator normalized to half unit mass [5]. The *energy demodulation of Mixtures* (EDM) algorithm developed in [5] uses these HOEO's to accomplish separation and demodulation of two component AM–FM signals, while the PASED algorithm uses the ESA in conjunction with algebraic separation to accomplish multicomponent AM-FM signal separation and demodulation [8]. For the sake of brevity, we will adopt the model and performance measures described in [5]. The underlying assumption is that the component IF/IA signals vary slowly and little compared to their carriers [6].

4. ENERGY DEMODULATION OF CPM SIGNALS

The optimal demodulation approach for CPM signals is ofcourse the maximum likelihood approach embodied in the Viterbi algorithm [1], but the computational complexity of this method in terms of the number of phase states is pM^{L-1}, where M is the alphabet size of $a[k]$ [1]. Several suboptimal variants of the Viterbi algorithm and other approaches to the CPM demodulation problem are described in [1, 3]. Our goal here is to formulate the CPM demodulation problem in the AM–FM framework of the energy operator and to develop a framework for simpler suboptimal energy-related approaches to CPM signal demodulation.

For monocomponent CPM demodulation, we employ the multiband–ESA [9] with FIR linear phase multiband filters of order 31. Although we implicity perform FM demodulation, for this application our interest is in the capability to detect the correct bits. The detector used subtracts the carrier frequency from the IF estimate and employs matched filtering with sign detection. We compare the average probability of symbol error averaged over 100 experiments obtained via the use of the MESA with the detection error for binary antipodal modulation in AWGN as given by [3]:

$$\Pr(\epsilon) = Q\left(\sqrt{2\frac{E_b}{N_o}}\right),$$

where $Q(.)$ is the standard normal tail probability. The corresponding expression for $MARY - PAM - AWGN$ detection is given by:

$$\Pr(\epsilon) = \frac{2(M-1)}{M} Q\left(\sqrt{\frac{6\log_2(M)E_{av}}{(M^2-1)N_o}}\right),$$

where E_{av} is the average energy per bit [3]. Simulations results shown in Fig. (1)(a,b) indicate that for a SNR/bit threshold around $\gamma_c = 5 - 7$ dB the MESA–based demodulator becomes error free and completely inverts the effects of CPM modulation. Simply increasing the modulation index h will increase the strength of the signal modulations in the IF signal and will consequently improve the performance of the algorithm to a certain extent as seen from Fig. (4)(a,b,c) where the modulation indices were $h = 0.025, 0.05, 0.1$ respectively. This approach is however, valid only when the modulation indices are in the region where the narrowband AM–FM approximation holds [6]. In comparison maximum likelihood detection forbids the use of specific weak values of the modulation index h, where the minimum distance between phase states is small [2]. We can further observe from Fig. (4)(c) that 1-REC-CPM slightly outperforms 1-RAC-CPM, due to the fact that the signal modulation strength is more, but at the expense of spectral compactness due to the presence of larger side-lobes in the power spectrum of the CPM signal [1].

Fig. (2) describes a 4-PAM-CPM example, where the CPM signal with parameters $h = 0.04$, $L = 1$, and SNR $= 13$ dB is described in Fig. (2)(b). The normalized IF estimates of the ESA with 6-time binomial smoothing (SESA) of the energy signals in the ESA over 20 symbol intervals are described in Fig. (2)(b). In Fig. (2)(c) compares the performance of the SESA for $M = 2$ and $M = 4$ with the performance of a $4 - PAM$ detector in AWGN [3]. Since the number of alphabet levels is increased to $M = 4$, i.e., $a[k] \in \{\pm 3, \pm 1\}$, the bandwidth of the resultant CPM increases and the narrowband approximation used in [6] becomes less valid resulting in a larger error for $M = 4$.

Consider a two-component CPM signal environment in Fig. (3), where the components are both 1-REC-CPM signals with modulation indices $h_1 = h_2 = 0.04$, $T_b = 5ms$ and $f_s = 10$ kHz, *normalized carrier separation* (NCS) parameter [5] of 0.8 and a relative power ratio (MPR) of 0 dB. With this parameter setting, there is a significant amount of spectral overlap. CPFSK demodulation is accomplished using the MESA algorithm, where the FIR multiband filters of order $L_{\text{ord}} = 31$ employed were designed using the

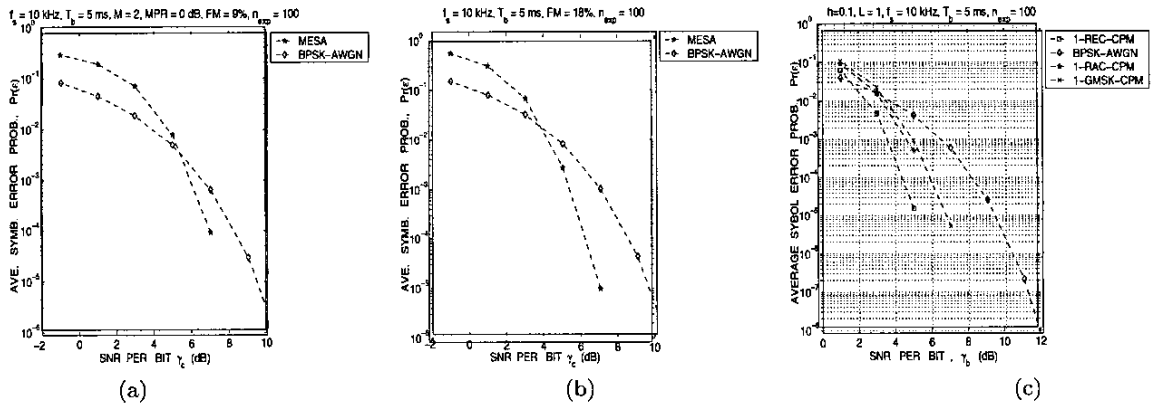

Figure 1: CPM monocomponent demodulation: (a) performance of the MESA versus BPSK-AWGN detection for $h = 0.025$ and $L = 1$ (FM = 9%), (b) performance of the MESA for $h = 0.05$ and $L = 1$ (FM = 18%), (c) performance of the MESA for the parameters $h = 0.1$ (FM = 36%) and $L = 1$ using FIR filters of order 31 for 1-REC-CPM, 1-RAC-CPM and 1-GMSK-CPM.

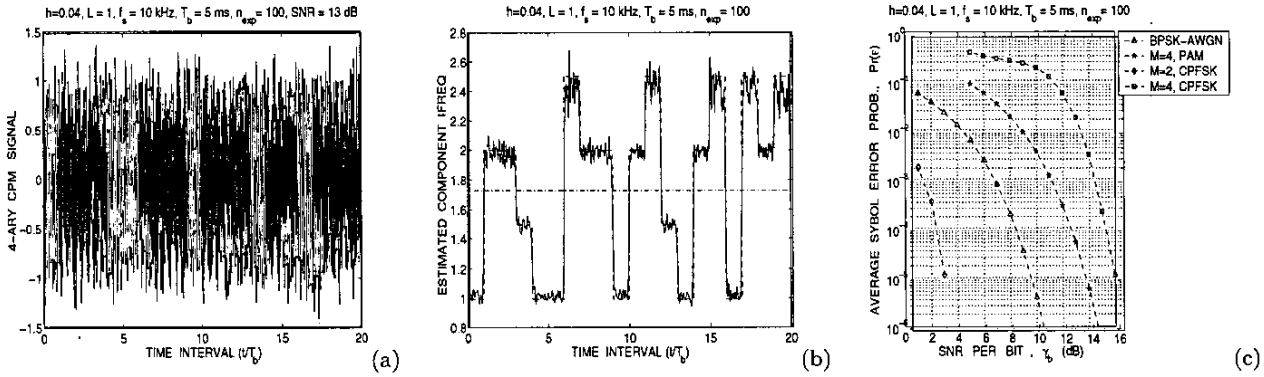

Figure 2: M-ARY-CPM monocomponent demodulation: (a) M=4 CPM signal using a rectangular pulse shaping function, (b) normalized IF estimates of the ESA using 6-time binomial smoothing of the energy signals, (c) performance of the smoothed-ESA (SESA) for $M = 2$ and $M = 4$. Estimates are solid lines, dashed lines are actual quantities, and dashed-dotted lines are carrier frequency estimates.

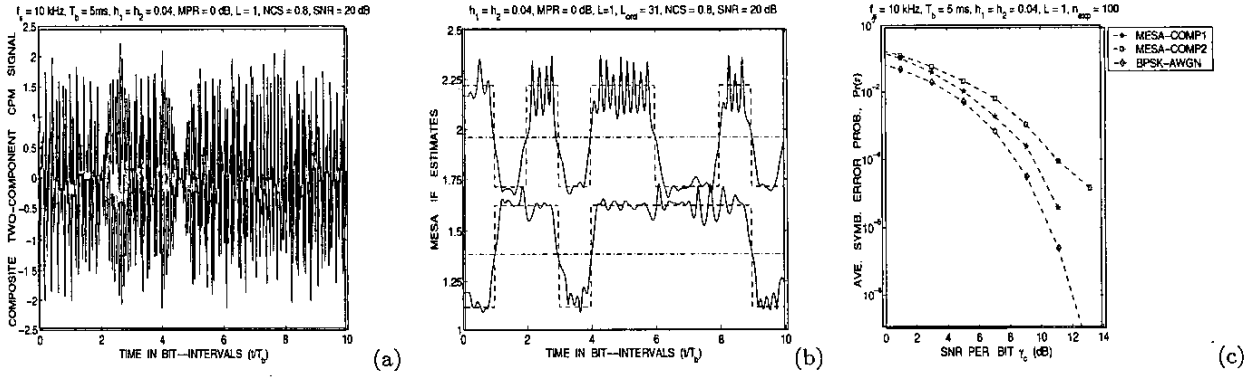

Figure 3: Two-component CPFSK demodulation using the MESA algorithm: (a) Composite CPFSK signal over 10 bit intervals, (b) corresponding MESA IF estimates using FIR filters of order $L_{\text{ord}} = 31$ designed using the window method, where the dashed lines are the actual IF's and the dashed-dotted lines are the MESA carrier frequency estimates, (c) comparison of the average probability of symbol error of the MESA algorithm averaged over 100 experiments with that of binary detection in AWGN.

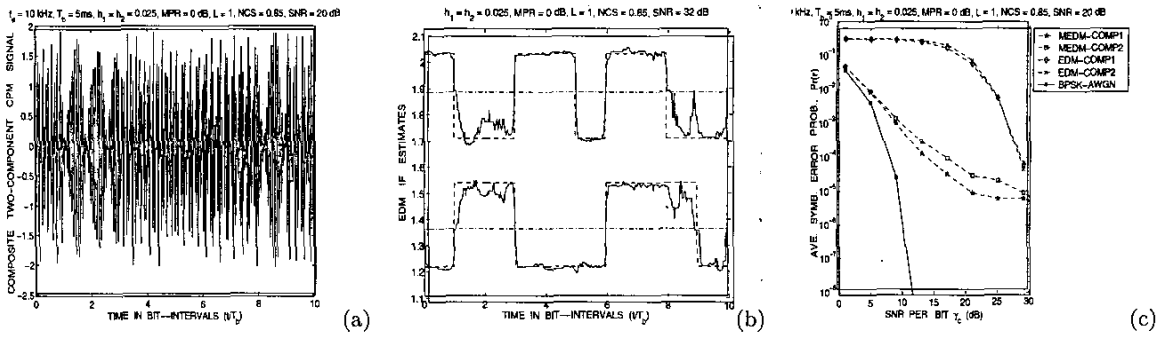

Figure 4: Two-component CPFSK demodulation: (a) Composite CPFSK signal over 10 bit intervals, where the modulation indices of the components are $h_1 = h_2 = 0.013$ (b) corresponding MEDM IF estimates, where dashed lines denote actual quantities and dashed-dotted lines denote carrier frequency estimates, (c) comparison of the average probability of symbol error of the EDM algorithm with 11-pt median IF–smoothing and the related MEDM algorithm.

window method. Fig. (3)(b) describes the MESA IF estimates with 6-time binomial smoothing of the constituent energy signals. Fig. (3)(c) compares the performance of the MESA algorithm with that of binary detection in AWGN and indicates that the two-component CPM demodulation problem is equivalent to two mono-component demodulation problems when the components are spectrally separated and simple bandpass filtering is sufficient to separate them. As the spectral separation between the components decreases, the filters needed to separate the components become intractable.

Now consider a two-component adjacent channel interference (ACI) situation, where the received signal contains two CPFSK-modulated components, where one of the components models the *signal of interest* (SOI) and the other models the interference. The relative power ratio between the components is 0 dB and the NCS parameter is approximately 0.85. With this parameter setting, the components have significant overlap. Fig. (4) (a,b) describe the composite CPM signal and the IF estimates of the EDM algorithm for a SNR of 40 dB. In Fig. (4) (c) we compare the average probability of symbol error from averaging over 100 experiments obtained via the application of the EDM and the *multiband-EDM* (MEDM). As expected, the MEDM algorithm, that employs energy detection and multiband filtering, performs better than the regular EDM algorithm at lower SNR's but incurs more errors at higher SNR's due to the effects of filtering [9]. Furthermore note that the energy demodulation approaches are robust to a Doppler shift in the data which will simply manifest as a constant shift in the IF estimates [4] that can be subtracted out.

5. CONCLUSIONS

In this paper, we applied the energy-operator related mono-component and multicomponent demodulation approaches that have traditionally been applied to problems arising in speech formant demodulation and image texture analysis applications to the problem of CPM demodulation. The digital phase modulation schemes derived from CPM were cast into the AM–FM signal framework required by the energy-based approaches. Simulation results show that these energy related methods are particularly suitable for binary modulation schemes. These approaches are also robust to the presence of Doppler shifts. These techniques albeit suboptimal compared to the Viterbi algorithm approach provide a computationally simpler alternative to the CPM signal demodulation problem.

REFERENCES

[1] C-E. W. Sundberg, "Continuous Phase Modulations Part I and II," *IEEE Commun. Magazine*, Vol. 24, pp. 25-38, April 1986.

[2] J. B. Anderson, T. Aulin and C-E. W. Sundberg, "Digital Phase Modulation," Plenum, New York, 1986.

[3] J. G. Proakis, "Digital Communications," fourth edition, McGraw-Hill Companies, Inc., New York, 2001.

[4] S. Barbarossa and A. Scaglione, "Demodulation of CPM Signals Using Piecewise Polynomial Phase Modeling," *Proc. ICASSP-98*, Vol. 6, pp. 3281-3284, 1998.

[5] B. Santhanam and P. Maragos, "Energy Demodulation of Two–Component AM–FM Signal Mixtures," *IEEE Sig. Process. Lett.*, vol. 3, pp. 294-298, Nov. 1996.

[6] P. Maragos, J. F. Kaiser, and T. F. Quatieri, "On Amplitude and Frequency Demodulation Using Energy Operators," *IEEE Trans. Sig. Process.*, vol. 41, pp. 1532-1550, April 1993.

[7] B. Santhanam and P. Maragos, "Energy Demodulation of Two-Component AM-FM Signals with Application to Speaker Separation," *Proc. of ICASSP-96*, Vol. 6, pp. 3517-3520, Nov. 1996.

[8] B. Santhanam and P. Maragos, "Multicomponent AM-FM Signal Separation and Demodulation Via Periodicity-based Algebraic Separation and Energy-based Demodulation," *IEEE Trans. on Commun.* Vol. 48, No. 3, pp. 473-490, 2000.

[9] A. C. Bovik, P. Maragos, and T. F. Quatieri, "AM–FM Energy Detection and Separation in Noise using Multiband Energy Operators," *IEEE Trans. Sig. Process.*, Vol. 41, pp. 3245-3265, Dec. 1993.